Materials Characterization 118 (2016) 560–569

Contents lists available at ScienceDirect

Materials Characterization

journal homepage: www.elsevier.com/locate/matchar

SEM and TEM characterization of microstructure of stainless steel composites reinforced with TiB_2

Iwona Sulima [a,*], Sonia Boczkal [b], Lucyna Jaworska [a]

[a] Institute of Technology, Pedagogical University of Krakow, Podchorążych 2 st., 30-084 Krakow, Poland
[b] Institute of Non-Ferrous Metals in Gliwice, Light Metals Division, Skawina, Poland

ARTICLE INFO

Article history:
Received 13 November 2015
Received in revised form 31 May 2016
Accepted 6 July 2016
Available online 6 July 2016

Keywords:
Microstructure
Complex boride
Phase
Composite
Spark Plasma Sintering (SPS)
High Pressure-High Temperature (HP-HT) sintering

ABSTRACT

Steel-8TiB_2 composites were produced by two new sintering techniques, i.e. Spark Plasma Sintering (SPS) and High Pressure-High Temperature (HP-HT) sintering. This study discusses the impact of these sintering methods on the microstructure of steel composites reinforced with TiB_2 particles. Scanning electron microscopy (SEM), wavelength dispersive spectroscopy (WDS), X-ray diffraction, electron backscatter diffraction (EBSD) and transmission electron microscopy (TEM) were used to analyze the microstructure evolution in steel matrix composites. The results of microscopic examinations revealed a close relationship between the composite microstructure and the methods and conditions of sintering. Substantial differences were observed in the grain size of materials sintered by HP-HT and SPS. It has been demonstrated that the composites sintered by HP-HT tend to form a chromium-iron-nickel phase in the steel matrix. In contrast, the microstructure of the composites sintered by SPS is characterized by the presence of complex borides and chromium-iron phase.

1. Introduction

Powder metallurgy (PM) is considered one of the key technologies for the fabrication of composites reinforced with ceramic particles [1,2]. Compared with other methods, its undeniable advantage is better control of microstructure, allowing for a uniform distribution of the reinforcing phase in sintered composite [3–5]. Sintering by conventional methods takes a long time and requires high temperature, both of which produce sinters of high density. However, the long time of sintering causes grain growth and loss of the unique properties resulting from the fine-grained microstructure of a composite material [6–8]. The use of modern sintering technology allows reducing both time and temperature of the sintering process with positive impact on the economic aspect of the fabrication of composite materials. Both HP-HT and SPS techniques are included in the group of modern advanced technologies. Application of technologies in which different mechanisms control the sintering process can affect the composite microstructure and, as a further consequence, its physical, mechanical and functional properties [9]. Compared with the conventional sintering process, HP-HT offers several quite unique advantages, to mention only energy savings, shorter time of sintering (a few minutes only), full consolidation of the sintered material, and suppressed grain growth [10,11]. In addition to the aforementioned benefits, the widespread use of SPS is also the matter of the economic viability of this process, resulting partly from the lower temperature and partly from the shorter time of sintering. In this method, heating of the sintered powder is done with pulse current. During flow of this current, sparks are generated in pores of the sintered material, removing particles of adsorbed gases and oxides from the surface. This facilitates active contact between particles of the sintered powder. Consequently, this and other similar phenomena shorten the time and reduce the temperature of the sintering process [12,13].

Recent years have witnessed a growing interest in iron alloys, mainly due to their potential applicability as a matrix of the composite materials. The main factors that decide about this fact include the low cost of production, high mechanical properties of iron alloys and satisfactory corrosion resistance. Compared with aluminium and its alloys, iron-based alloys, austenitic steels - in particular, offer higher strength, better stiffness and ductility [14]. The ceramic particles most commonly used as a reinforcement of the steel matrix are oxides (Al_2O_3, ZrO_2), nitrides (TiN, Si_3N_4), carbides (TiC, Cr_3C_2, VC, B_4C) and borides (TiB_2, ZrB_2) [15–22]. Abenójar et al. [23] studied the effect of the type and content of the reinforcing phase ($AlCr_2$, Cr_2Ti, VC and SiC) and sintering atmosphere on the microstructure and properties of 316L stainless steel matrix composites. It has been demonstrated that the use of intermetallic phases is a good way towards the achievement of improved properties of the composites tested. Akhtar et al. [24] analyzed the effect of $MoSi_2$ addition on the sintering behavior and microstructure evolution of sintered 316L stainless steel. It was found that $MoSi_2$ dissociated during sintering

* Corresponding author.
E-mail address: isulima@up.krakow.pl (I. Sulima).

http://dx.doi.org/10.1016/j.matchar.2016.07.005
1044-5803/

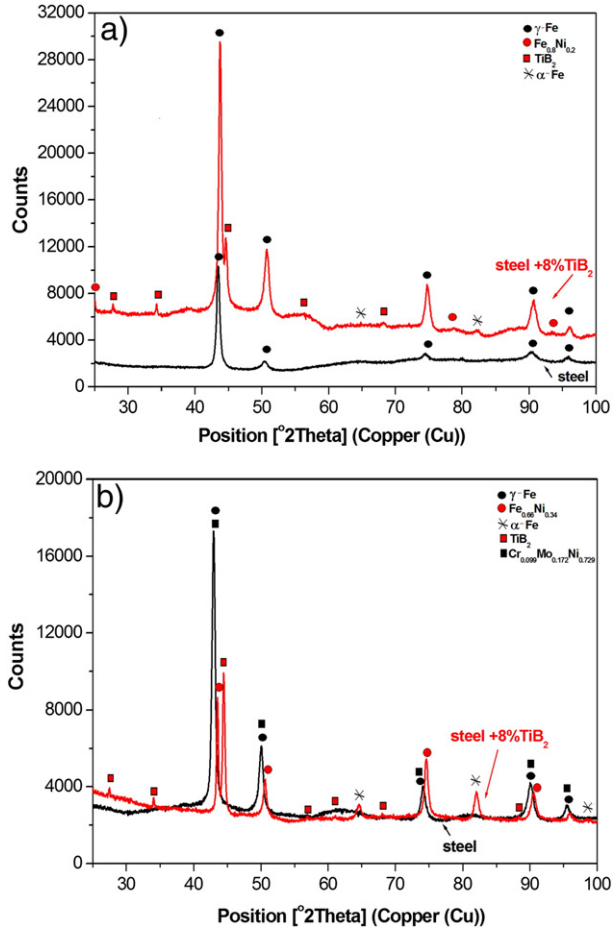

Fig. 1. XRD patterns of sintered 316L steel and composites steel-8TiB_2: a) HP-HT method (1300 °C-7 GPa) and b) SPS method (1100 °C-30 min).

with the resulting segregation of Mo and Si at grain boundaries. Excessive amounts of Mo and Si appeared as separate phases in the microstructure. The addition of $MoSi_2$ to 316L stainless steel was observed to increase the density, hardness and tensile strength of this steel after sintering. On the other hand, Jain et al. [25] have proved that the addition of 5 wt% of YAG improves both density and hardness of the sintered ferritic and austenitic steels. The effect of YAG particles on the compaction process is definitely enhanced by the sintering process carried out at 1400 °C. In turn, Akhtar et al. [26] sintered 465 steel with the addition of Si_3N_4. Tests covered the stability of the Si_3N_4 phase in a steel matrix. It has been shown that the increasing content of Si_3N_4 phase increases the sintered density. The maximum theoretical density of 98.5% was obtained in the composite containing 5 wt% of Si_3N_4, but it was found that particles of Si_3N_4 are stable in the steel matrix only up to the content of 2 wt%. Higher content of Si_3N_4 dissolves the ceramic phase in the matrix. Patankar and Tan [18] studied 316L stainless steel reinforced with SiC. They proved that adding SiC to this steel allowed obtaining higher densities of the sintered material. This effect was attributed to reactions occurring between the SiC phase and steel matrix at 1100 °C giving rise to the formation of a low melting Fe-SiC phase.

The aim of this study was to investigate the effect of two sintering methods on changes in the microstructure of steel-8TiB_2 composites. Titanium diboride was selected as a steel matrix reinforcement owing to its low density, very high hardness, high strength at elevated temperatures, and good thermal stability and wettability [27]. Several authors produced steel composites reinforced with TiB_2 by the technique of powder metallurgy using conventional sintering and hot isostatic pressing (HIP) [28–30]. The techniques selected in this study for the manufacture of steel-8TiB_2 composites included two modern advanced techniques, i.e. Spark Plasma Sintering (SPS) and High Pressure-High Temperature (HP-HT) sintering.

2. Methods

Commercially available TiB_2 powder (H.C.·Starck) and 316L steel powder (99.9 wt.%, Hoganas) were used in these studies. The stainless steel powder had the following chemical composition: 17.20 wt% Cr, 12.32 wt% Ni, 2.02 wt% Mo, 0.43 wt% Mn, 0.89 wt% Si, 0.03 wt% S, 0.028 wt% P, 0.03 wt% C and Fe as a balance. The average particle size of TiB_2 and AISI 316L steel powders was 2.5–3.5 μm and 25 μm, respectively. The raw powders were mixed for 8 h in a TURBULA mixer. For the sintering process, a composite mixture of powders of the 316L steel + 8 vol% TiB_2 was prepared.

Composites were sintered by the HP-HT and SPS techniques. In the case of SPS, the composite mixture was fed into a cylindrical graphite mould with an inner diameter of 20 mm. The sintering process was carried out in SPS HP5 equipment made by FCT (Germany). The following sintering parameters were observed: temperature - 1100 °C, pressure - 35 MPa, and heating rate - 200 °C/min. The sintering time was 5 and 30 min. The sintering temperature was measured with a pyrometer (IGA-5). The height of the sintered samples was 7 mm. In the HP-HT process, disk-shaped samples with a diameter of 15 mm and a height of 4 mm were used. The samples were first cold-pressed in a steel die under a pressure of 100 MPa. Next, the process of sintering was carried out using a toroidal Bridgman-type apparatus. The sintering temperature and time were 1300 °C and 60 s, respectively. Two sintering pressures of 5 and 7 ± 0.2 GPa were applied.

Composite microstructure was examined by scanning electron microscopy (SEM) using a new concept, ultra high-resolution, Hitachi SU-70 scanning electron microscope equipped with a field emission gun and a set of Thermo detectors. Chemical analysis of sintered materials was made by WDS. The X-ray diffraction patterns were obtained using PANalytical Empyrean diffractometer with copper radiation. The phase identification was done with the ICDD (PDF4 + 2015) files. The quantitative phase analysis of the examined composites was performed by the Rietveld refinement using HighScore PANalytical software.

Phase analysis and analysis of the crystallographic orientation of grains were performed under a high-resolution INSPECT F50 FEI

Table 1
List of phases identified in the composites sintered by SPS and HP-HT.

Ref. code	Compound name	Chemical formula	Crystal system	Space group
01-089-4185	Iron	γ-Fe	Cubic, a = 3.6468 Å	Fm-3 m
04-014-0258	Iron	α-Fe	Cubic, a = 2.8700 Å	Im-3 m
04-002-3697	Iron-nickel	γ-$Fe_{0.66}Ni_{0.34}$	Cubic, a = 3,6040 Å	Fm-3 m
04-015-0310	Iron-nickel	γ-$Fe_{0.8}Ni_{0.2}$	Cubic, a = 3,5830 Å	Fm-3 m
04-015-0503	Chromium-molybdenum-nickel	$Cr_{0.099}Mo_{0.172}Ni_{0.729}$	Cubic, a = 3.6100 Å	Fm-3 m
04-006-2019	Titanium diboride	TiB_2	Hexagonal, a = 3.0190 Å, c = 3.2180 Å	P6/mmm